INFLUENCE OF FILLER WIRE ON MECHANICAL AND METALLURGICAL BEHAVIOUR OF INCONEL 690 ALLOY WELDED BY PULSED CURRENT GAS TUNGSTEN ARC WELDING

S.Sivalingam[1], G.Sureshkannan[2], D.Balaji[3], L.Rajeshkumar[4*]
[1, 2]Department of Mechanical Engineering, Coimbatore Institute of Technology, Coimbatore, Tamilnadu, India
[3, 4]Department of Mechanical Engineering, KPR Institute of Engineering and Technology, Coimbatore, Tamilnadu, India
[1]sivalaiyaa@gmail.com, [2]sureshkannan.mech.cit@gmail.com, [3]balaji.ntu@gmail.com

Abstract

Metal corrosion in higher temperature due to stress is the common phenomenon. In order to reduce this issue the nickel based alloys play an imperative role, particularly super alloy 690 is a remarkable one. This is due to the presence of overall chromium content of around 30 % and this shows the much better dominance in resisting corrosion. During welding the microsegregation of chromium is not recommended to be portrayed as a higher constituent. This is being inundated by using fillers like ERNiCrFe-7 (I-52) and ERNiCr-3 (I-82) by using pulsed current gas tungsten arc (PCGTA) welding, which reduces the microsegregation of chromium carbides in the weldments. The segregation is analyzed using scanning electron microscopy (SEM) which reveals that there is no microsegregation in both the weldments (ERNiCrFe-7 and ERNiCr-3) which leads to the formation of fine grains. Specifically, the weld center of both the weldments reveals the equiaxed dendrites. This microsegregation is contributing to the mechanical properties which is being ensured by tensile and impact examination that depicts the strength and toughness of I52 (681 MPa and 68.3 J) weldments are greater than the I82 (662 MPa and 67 J) weldments and both are in turn higher than the base metal in strength.

Keywords: *Inconel 690; ERNiCrFe-7; ERNiCr-3; Tensile Strength; Impact strength*

1. Introduction

The construction of pressurized water reactor (PWR) system in the nuclear power plant faces consistent problems due to the corrosion failure. Initially the pressure water tube was made out of stainless steel SS304. This material could not sustain for long period of time owing to the severe attack of stress corrosion cracking (SCC). This issue urges for new material and so the alloy 690 was identified alternate to SS304 [1]. Alloy 690 is a solid solution strengthened nickel based super alloy and it was derived from Ni-Cr-Fe ternary system. The presence of higher chromium content provides the outstanding resistance to oxidizing chemicals and gases. Nickel imparts resistance to stress corrosion cracking in chloride environments. Alloy 690 is widely used in steam generator tubes in nuclear power generation reactor system in line for their appreciable property [2]. Lee and Kuo (1999a) examined alloy 690 weldments, for their mechanical properties and microstructure, fabricated using filler metals I82 and I52 and they observed that the presence of TiN precipitates in both filler materials and also observed the presence of

* Corresponding Author: lrkln27@gmail.com

rich chromium carbides (Cr23C6) in the fusion zone of I82 weldments. The formations of precipitates affect the quality of weldments [3]. Aforementioned authors analyzed alloy 690 weldments in terms of the joining properties which was influenced by the filler metal composition. They observed the formation of M23C6 and C23C6 in the interdentritic regions of the weldments [4].

The researchers often focus on the precipitation development on weldments as it decides the strength of the weldments. The chromium carbide precipitation is developed due to the cooling rate of the weldments and this formation specifically occurs due to enormous heat supply to the fusion zone and heat affected zone which is susceptible to form the chromium carbides. The heat supply is continuous and high during GTAW process [5 - 10]. Jeng et al. (2007) also examined the chromium carbide precipitation formation in the dissimilar metal combination and they have adopted GTAW process [1]. They have tested the combination of INCONEL 690 with stainless steel SUS 304L and they examined the weldments which revealed Titanium, chromium and nitride precipitation in the weldments. It is observed from the reported literatures that the major problem encountered in the alloy 690 is the formation $Cr_{23}C_6$ and $M_{23}C_6$. Seclusion of chromium and some other alloying elements led to the formation of such phases. The authors believed that owing to development of welding method to prelude the segregation of alloying element chromium. The microsegregation of alloying element can be reduced by proper selection of matching filler wire and suitable welding technique. In this present study, author employed ERNiCr-3 and ERNiCrFe-7 as filler wires during the welding process. These filler wires are widely used in the industrial practice to weld alloy 690 [2]. A study reported by Srikanth and Manikandan (2017) on alloy 600 about a family of Ni-Cr-Fe based super alloy similar to alloy 690 used a filler wire I-82 to fabricate weldments on GTAW and PCGTAW welding process. They also concluded that, when swapping between GTAW and PCGTAW process extent of micro segregation chromium is completely suppressed. No traces of formation of M23C6 chromium rich phases were observed in the weldments [11]. Many other studies on different nickel based super alloys have shown that the pulsed current gas tungsten arc welding superior in the metallurgical and mechanical properties of the weld joint by reducing the extent of micro segregation. Some studies tried the various ways to control the effects of microsegregation by fabricating the weldments with PCGTAW method with three filler wires namely ERNiCrMo-10, ERNiCrMo-4 and ERNiCrMo-14. Examination at the macro level was done to disclose welded joint defects. Similarly, micro level attributes like fusion zone (FZ) and heat affected zone (HAZ) were examined under optical and scanning electron microscopy [12].

Many researchers have carried out works on PCGTA welding also, which were consolidated as follows. Hadadzadeh et al. (2014) reported while carrying out the PCGTA welding for alloy 617, compared their process with GTAW and the results revealed that FZ microstructure tweaked and there is a substantial enhancement in the toughness of the material when switching over between the GTAW and PCGTAW [13, 14]. The study on Ni–Fe–Cr base alloy 718 by comparing the welding process of GTAW and PCGTAW is being examined and the results depicts that PCGTAW lessened the adversity of segregation related to solidification and brought down the magnitude of harmful laves phase [15-17]. GTA and PCGTA weld specimen of the alloy C-276 were mechanically tested. Improvements accumulating for pulsed current welding microstructure and mechanical behavior were observed [18]. The Pulsed current welding has considerable advantages, like improved stability in arc generation, enhanced depth to width ratio of the weldments, superior grain size, porosity is less, distortion is less and controlled heat input over GTAW [19, 20]. Based on the reported literature there are

very few published study reported on the related quality of weldment produced in PCGTAW with a keen interest towards the extent of micro segregation. The aim of the present study is to bridge the gap explored from the above literature. It is also believed in the present study that the extent of microsegregation is dominated by switching over to PCGTA welding techniques to avoid the formation of Cr-rich precipitates.

2. Materials and Methods

Alloy 690 was acquired as hot rolled sheet with a thickness of 4 mm and then the spectroscopy test was carried out to find the base metal chemical composition as tabulated in table 1. Then the base metal was sliced into pieces for a dimension of 130 × 55 × 4 mm. The specimens were then cleaned using acetone in order to remove the dust particles in the base metal. After that, a single V-Butt was created with an angle of 45° and the pieces were held in a fixture to perform the welding. Before starting the welding process, bulging and shielding gases are supplied to the pieces at a rate of 15 l/min. Once this was done, the welding of sliced pieces has been done using KEMPII MIN ARC TIG machine. The welding has been done with certain process parameters and the amount of heat input given during welding process is listed in table 2. The heat input (HI) is expressed in kJ/mm (as in equation 2) for pulsed current welding and mean current (as in equation1) can be calculated using the following formula,

$$\mathrm{Im} = \frac{(Ip \times tp) + (Ib \times tb)}{(tp + tb)} amps \qquad (1)$$

$$HI = \frac{\mathrm{Im} \times V}{S} \times \eta\left(\frac{KJ}{mm}\right) \qquad (2)$$

Where I_m = Mean current, I_p = Pulse current, I_b = Base current, t_p = pulse current duration, t_b = background current duration, V = Voltage, S = Welding Speed

Table 1 Chemical composition of the base metal

Base metal	Chemical composition (wt. %)												
	Ti	C	Mn	P	S	Si	Cu	Cr	Fe	Al	Nb	Ni	Ta
Inconel 690	0.37	0.024	0.212	0.001	0.010	0.193	0.003	28.38	9.317	-	-	61.49	-
ERNiCr Fe-7	1.0	0.04	1.0	0.02	0.015	0.50	0.30	28.60	9.44	1.10	-	57.88	0.10
ERNiCr -3	0.75	0.10	2.75	0.03	0.015	0.50	0.50	20.16	3.0	-	2.50	67.0	2.70

After completing the welding the weld area was cleaned with the brush. The weld coupons were prepared, for testing the microstructure and mechanical property, by wire cut EDM process. The specimens were cut in accordance with the ASTM standards (E8/E-8M-13a) and then the mechanical properties like tensile and impact tests were performed to analyze the tensile strength and toughness of the material.

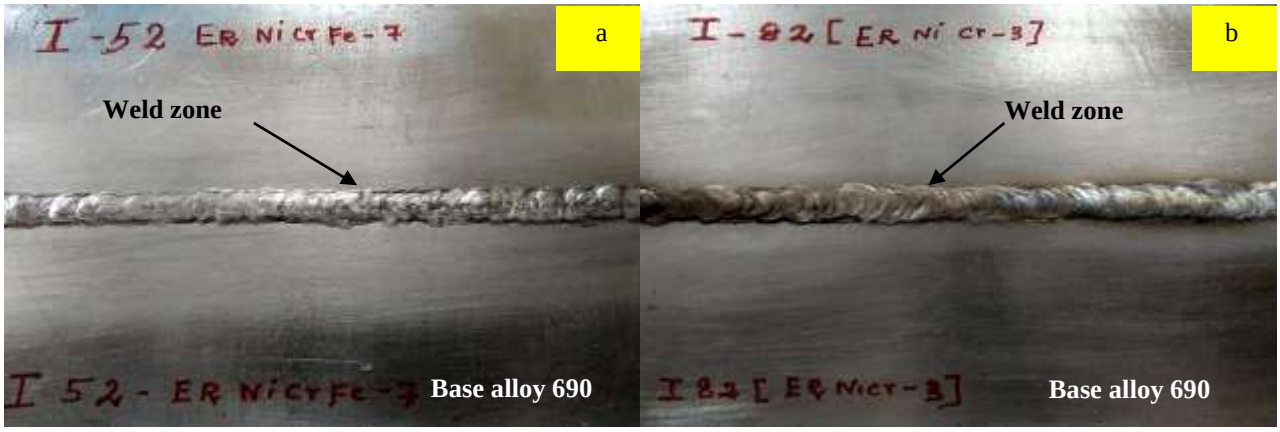

Figure 1. Photographic images of weldments made with (a) PCGTAW ERNiCrFe-7; (b) PCGTAW ERNiCr-3

Table 2 Welding process parameters

Specimen	Pass No	Welding Parameter				Total Heat Input (KJ min^{-1})
		Current (A)	Voltage (V)	Speed (mm s^{-1})	Heat Input (KJ mm^{-1})	
I52	1	70	11	1.226	0	0.922
	2	70	12	0.634	0.618	
	3	70	10	1.287	0.304	
I82	1	70	10	0.872	0	0.865
	2	70	11	0.828	0.473	
	3	70	12	1.000	0.392	

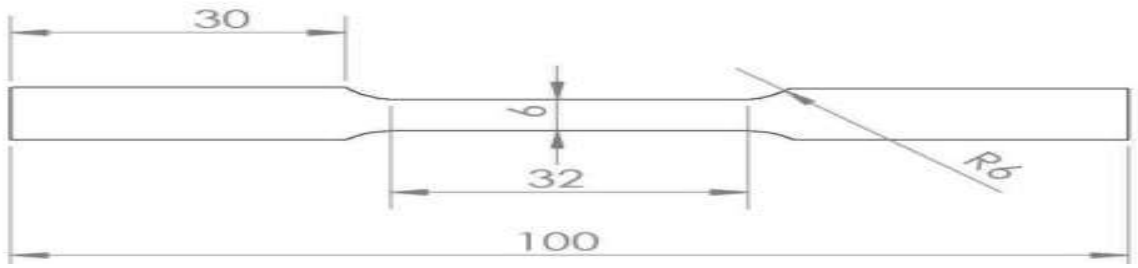

Figure 2. Schematic diagram showing the dimensions of tensile specimen

After that, the microstructure samples were polished by emery sheet ranging from 220 to 2000 silicon grit sheets followed by double disc polishing by alumina powder of 0.5 µm to remove the hard materials in the surface of the samples followed by electrolytic etching with 10 % oxalic acid for 45 s with 6 V to reveal the weld area on both the weldments. After that optical microscope was used to analyze the microstructure of the samples. Then the SEM/EDS analysis was performed to find the microsegregation in the weldments.

3. Results and Discussion

3.1 Macro Examination

Figure 3 illustrate the macro graph of weldments fabricated from alloy 690 with ERNiCrFe-7 and ErNiCr-3 as filler wires by PCGTA welding. The observed fluid flow in the macro graph indicated the steady fluid flow in the weld geometry. The effect of buoyancy force, Lorentz force and shear stress are clearly visible in the PCGTA weldments. The macrograph clearly shows that there were no defects observed in the weldment fabricated by the two different filler wires. It could be inferred from the macro graph that the process parameters employed in the present study is optimum to fabricate 4 mm thick plate of alloy 690.

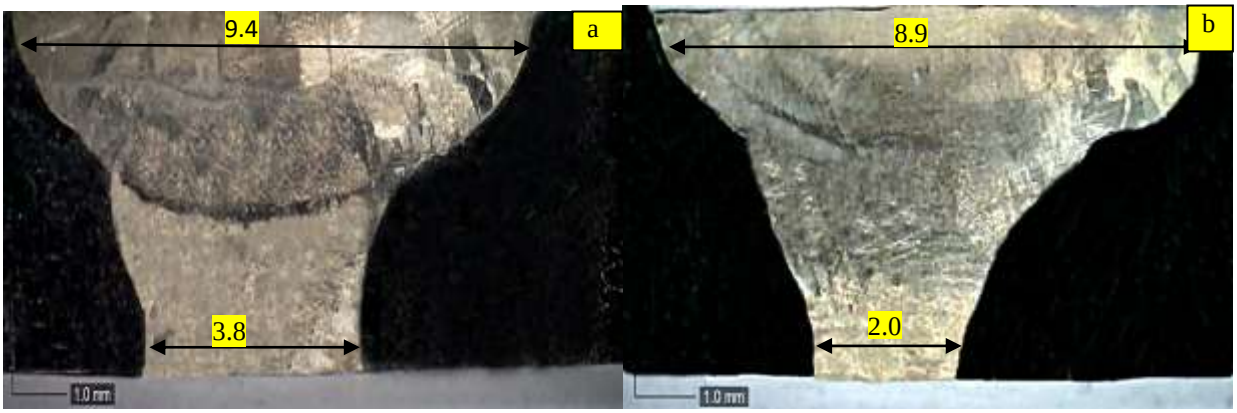

Figure 3. Macrostructure image of the weld joints (a) PCGTAW ERNiCrFe-7; (b) PCGTAW ERNiCr-3

3.2 Microstructure Examination

The solution annealed plates, which dissolves the carbon to prevent the formation of chromium carbide precipitates, were purchased. The presence of 61% of nickel in the alloy 690 renders uniformity among grains with austenitic structures. The microstructure of alloy 690 fabricated using filler wires ERNiCrFe-7 and ErNiCr-3 through PCGTA welding are shown in figures 4 and 5. Figures 4a & 4b represent the micro graph of weld centre and weld interface of ERNiCrFe-7 weldment. Similarly figures 5a & 5b shows the corresponding microstructure of ErNiCr-3 filler wire. The microstructure of both weldments depicts the fine equiaxed dendritic structure in the weld centre of the fusion zone (Figure 4a & 5a).

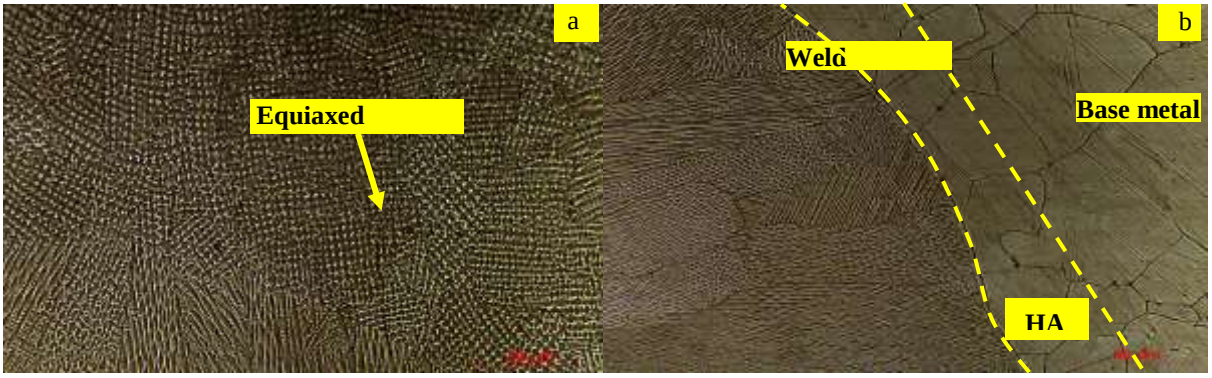

Figure 4. Optical microscopy of PCGTAW joints using ERNiCrFe-7 (a) weld center; (b) Weld Interface.

The micro graph of weld interface region shows the columnar dendritic structure. The microstructure close to the boundary line shows the planar structures. The variation in microstructure is due to the thermal gradient between the fusion boundary regions to the weld center. The fine equiaxed dendritic structure witnessed in the weld center of PCGTA weldments are due to the pulsing current variation employed during welding. During welding, melting of metal takes place at peak current and followed by cooling of molten metal achieved at base current due to which new grain growth takes place at weld zone

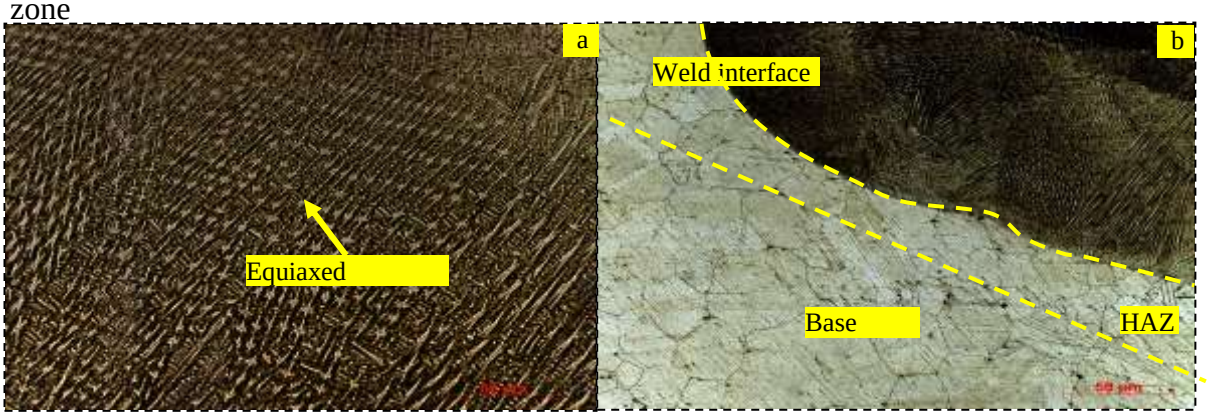

Figure 5. Optical microscopy of PCGTAW joints using ERNiCr-3 (a) Weld center; (b) Weld Interface.

As this process occurs continuously during welding, refinement of grain structure takes place in the weld zone of PCGTA weldments. From figure 4b and 5b it is observed that existence of unmixed zone were absent in the interface region of the weld zone due to the proper dilution of base metal and filler wires. It can also been seen from figure 4b and 5b that there were no difference in grain size observed between base metal and HAZ region.

3.3 SEM/EDS Analysis

Corresponding higher magnification of SEM micrograph for ERNiCr-3 is shown in figure 7a and 7b. It is observed from the SEM micrograph that secondary phases in the weldments fabricated by two filler wires were not present. Figure 6 (i-iv) shows the EDS analysis results of ERNiCrFe-7 and figure 7 (i-iv) shows the results for ErNiCr-3. The values of EDS analysis are also listed in the table 3 for ready reference. It is observed from both figures 6 and 7 that the segregation of Cr is not observed in both filler wires in the current analysis.

Lee et al reported the materialization of Cr23C6 phases observed in the GTA weldment of alloy 690 with filler wires ERNiCrFe-7 and ERNiCr-3. The composition of the Cr rich phases reported by Lee et al hasn't matched with the present study [3]. The authors confirm that the presence of Cr rich phases were suppressed and was revealed with the aid of line and elemental mapping of SEM/EDS as shown in the figure 8a and 8b.

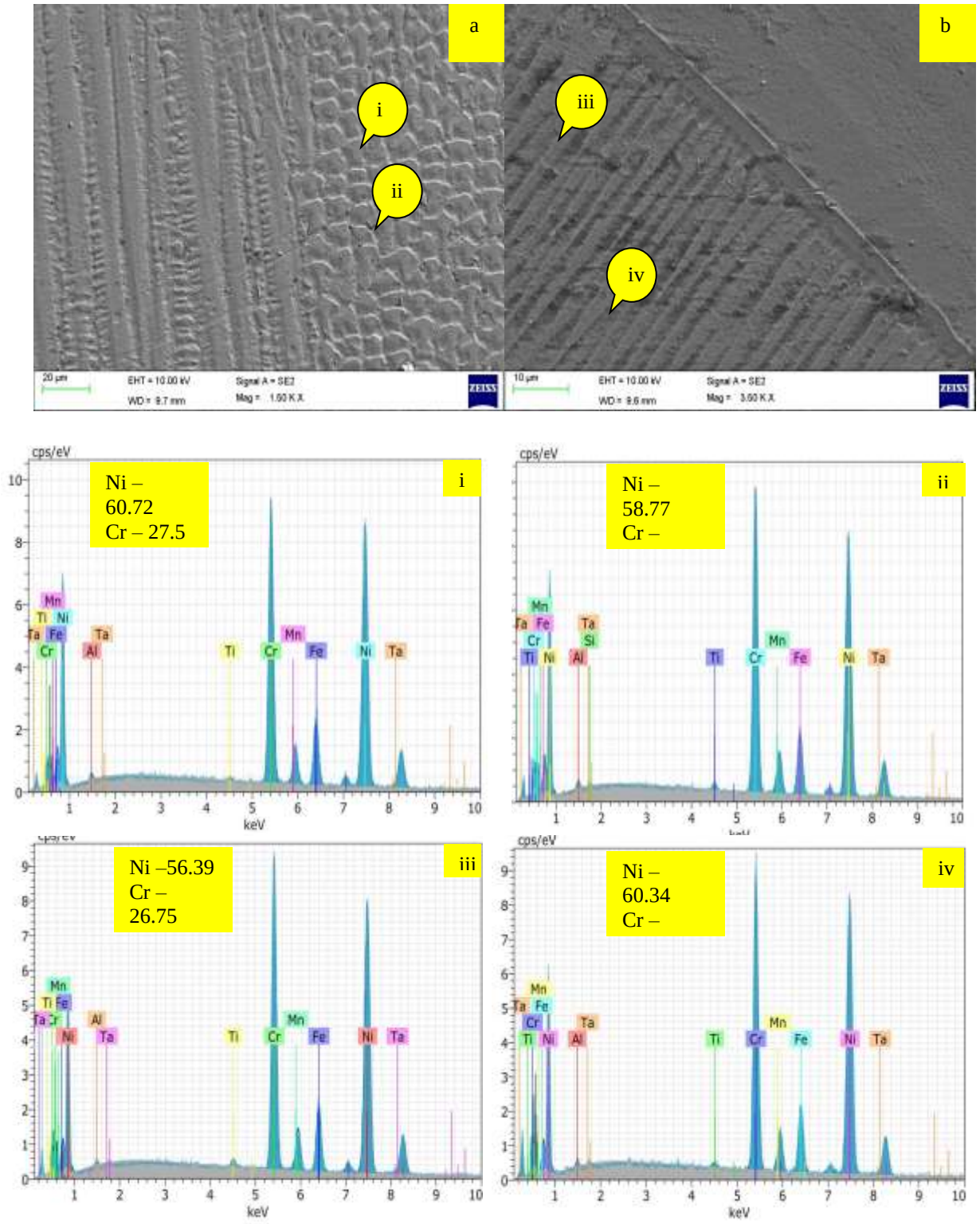

Figure 6. SEM/EDS analysis for ERNiCrFe-7 PCGTAW (a) SEM weld center ; (b) SEM weld interface ; (i) EDS of weld center dendritic core ; (ii) EDS of weld center interdendritic region ; (iii) EDS of weld interface dendritic core and (iv) EDS of weld interface interdendritic region

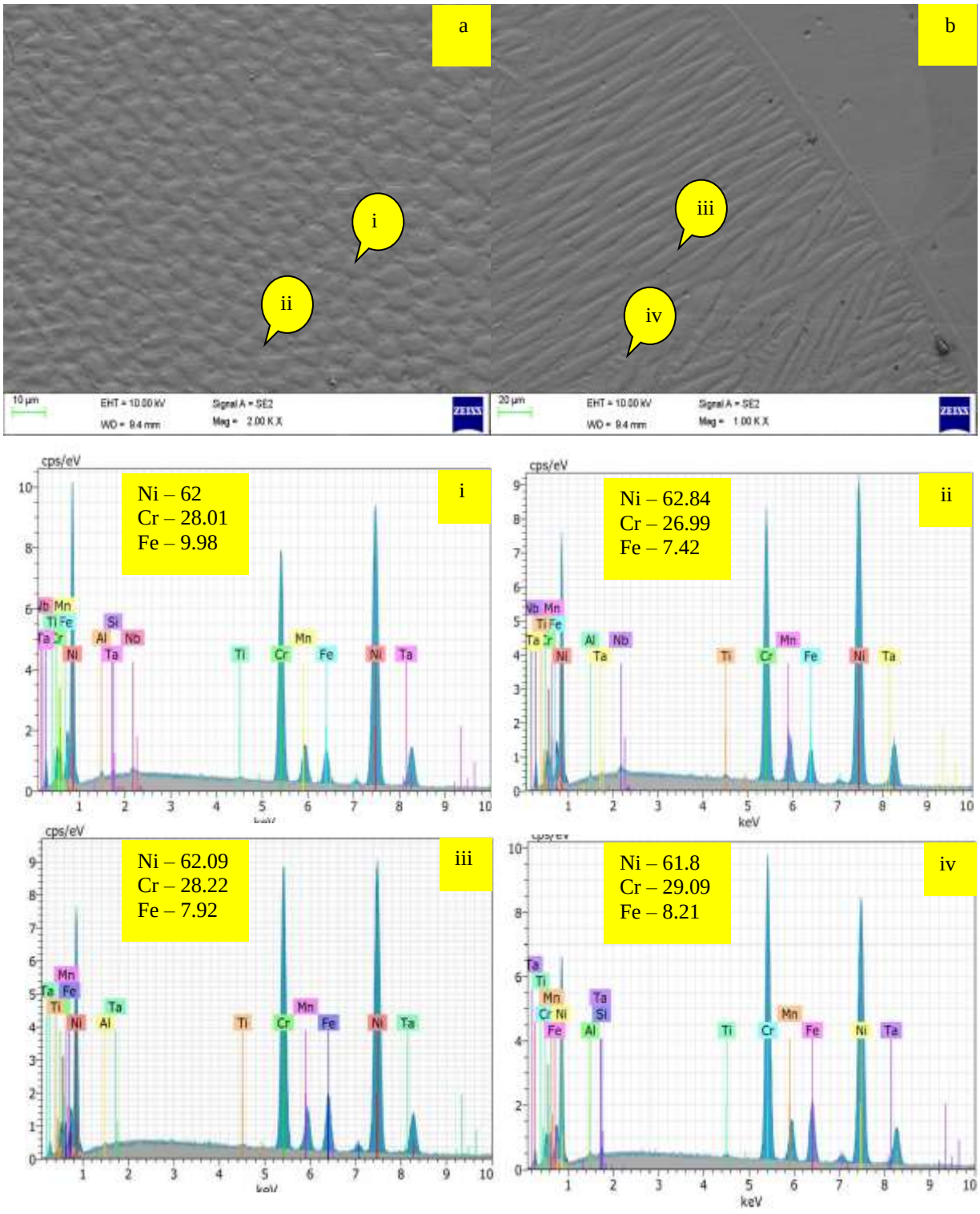

Figure 7. SEM/EDS analysis for ERNiCr-3 PCGTAW (a) SEM weld center ; (b) SEM weld interface ; (i) EDS of weld center dendritic core ; (ii) EDS of weld center interdendritic region ; (iii) EDS of weld interface dendritic core and (iv) EDS of weld interface interdendritic region

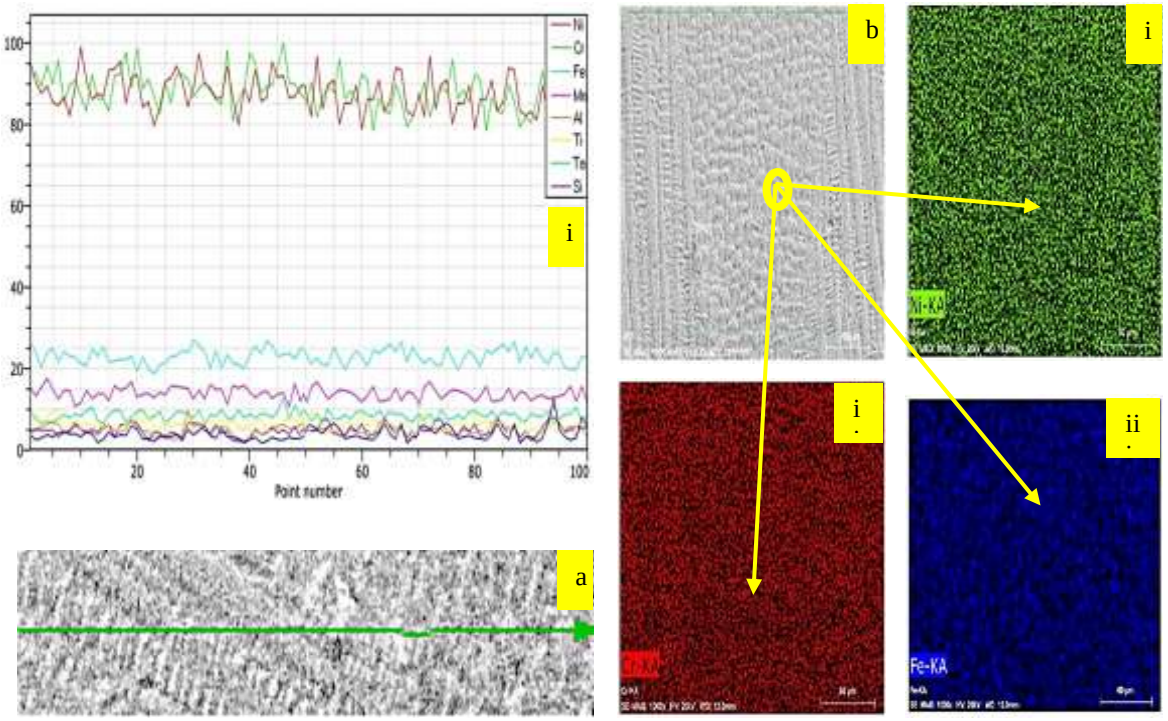

Figure 8a. Line and elemental mapping for ERNiCrFe-7 PCGTAW a. SEM/EDS image a. (i) SEM/EDS line mapping b. SEM/EDS image b. (i) Ni elemental mapping b.(ii) Cr elemental mapping b.(iii) Fe elemental mapping

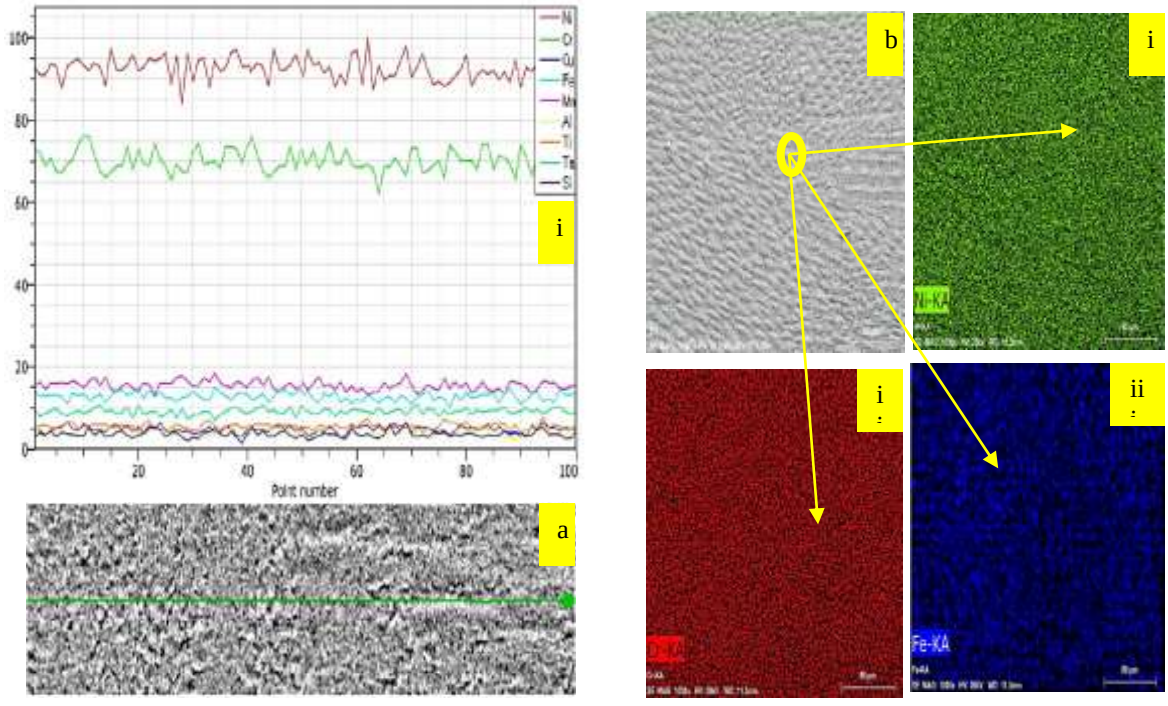

Figure 8b. Line and elemental mapping for ERNiCr-3 PCGTAW a. SEM/EDS image a. (i) SEM/EDS line mapping b. SEM/EDS image b. (i) Ni elemental mapping b.(ii) Cr elemental mapping b.(iii) Fe elemental mapping

Table 3. Elements levels in different zones in PCGTAW

Type of fillers	Zone	Ni	Cr	Fe
I52	Weld center dentritic core	60.72	27.5	9.69
	Weld center interdentritic region	58.77	29.11	9.25
	Weld interface dendritic core	56.39	26.75	8.63
	Weld interface interdentritic region	60.34	27.83	9.25
I82	Weld center dentritic core	62	28.01	9.98
	Weld center interdentritic region	62.84	26.99	7.42
	Weld interface dendritic core	62.09	28.22	7.92
	Weld interface interdentritic region	61.8	29.09	8.21

Authors calculated the tendency of micro segregation numerically with distribution coefficient (k) by using Scheil equation as shown in equation 2. Most of the researchers used this equation 3 to evaluate the micro segregation of alloying elements in different grades of nickel based super alloy.

$$k = \frac{Ccore}{Co} \qquad (3)$$

where C_{core} represents the elemental composition in dendritic core and C_0 represents the nominal composition of the base metal. When the value of k<1, it has a tendency for segregation at interdendritic region, whereas if the value of k>1, it has a tendency for segregation at dendritic regions. The table 4 shows that the k value of Ni, Cr and Fe are close to 1.This confirmed that extent of micro segregations were completely suppressed in the present study. PCGTAW ended up with faster cooling rate which rendered the absence of Cr-rich segregation. In the present study, authors has not carried out transmission electron microscope (TEM) analysis to confirm the presence of chromium carbide precipitates and it may be taken in near future. Based on EDS analysis authors conclude that presence of Cr-rich $Cr_{23}C_6$ phases absent in the present study.

Table 4. Elemental level at dendrite core zone at weld center (k)

Fillers	Ni	Cr	Fe
ERNiCrFe-7	0.98	0.96	0.951
ERNiCr-3	1.03	0.98	0.959

4. MECHANICAL TESTS

4.1 Tensile test

In order to assess the mechanical strength of the weldment, mechanical test was carried out. Table 5 shows the tensile test results obtained from weldments fabricated through PCGTA welding technique with two filler wires ERNiCrFe-7 and ErNiCr-3.

Table 5. Results of Tensile tests of weldments produced using the fillers ERNiCrFe-7 & ERNiCr-3

Welding process	Trial no	UTS (MPa)	Average UTS (MPa)
Alloy 690	637.9		
ERNiCrFe-7	1	680	681
	2	674	
	3	690	
ERNiCr-3	1	670	662
	2	650	
	3	665	

Figure 9 a and b shows the tensile failure samples of PCGTA weldments. The figures clearly reveal that failure was occurred in the base metal in the both weldments. The obtained tensile strength is greater than the base metal strength of alloy 690.

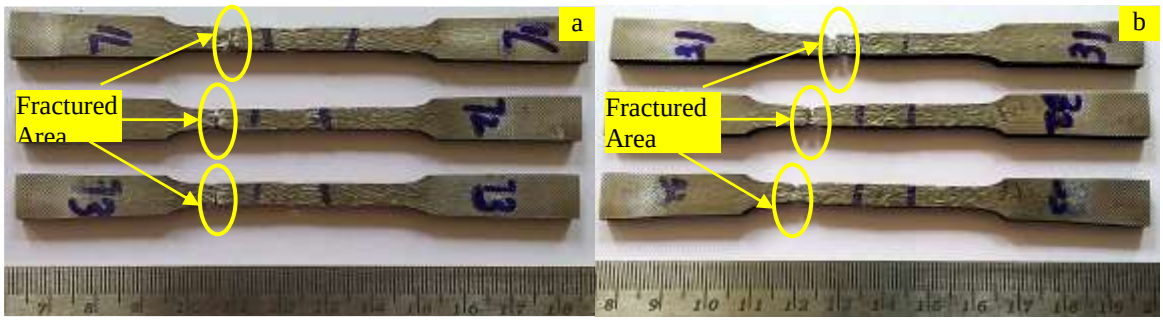

Figure 9. Photographs of tensile test of fractured specimen (a) PCGTAW ERNiCrFe-7; (b) PCGTAW ERNiCr-3

Figure 10 depicts the SEM micrograph of tensile failure samples. The presence of micro voids and dimples in the micrograph confirm the ductile mode of failure.

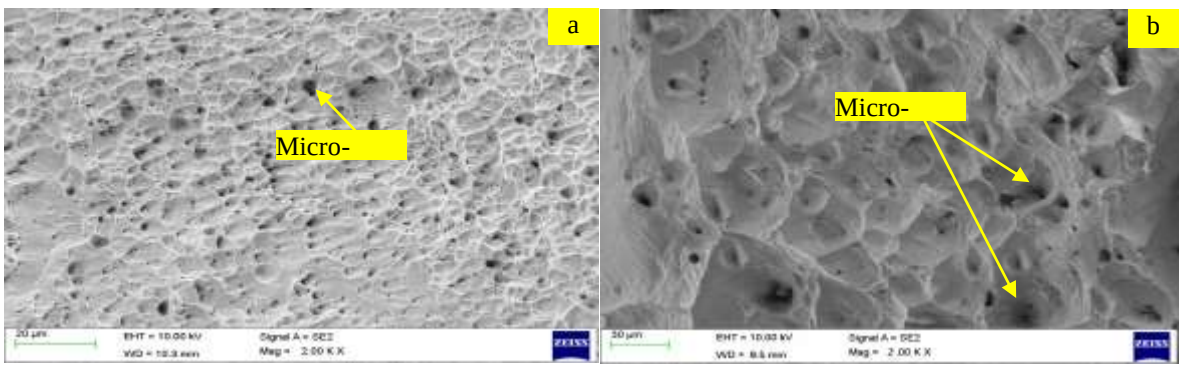

Figure 10. SEM Fractograph of tensile failure of PCGTAW (a) ERNiCrFe-7; (b) ERNiCr-3

4.2 Impact Test

Impact test was conducted on the three specimens for each of the welds to measure the ability of the object to resist sudden impact loading and the values were tabulated in Table 6. The specimens of the Pulsed current GTAW were found to have more ability to absorb energy. It could be observed from the table that the value of impact for weld specimen without filler was lesser than specimen welded using fillers. Specifically the impact value of specimen welded with ERNiCr-3 filler is higher than the impact value of ERNiCrFe-7 filler. This could infer a fact that segregation in PCGTA welded specimen by using fillers is very less when compared with GTA welded specimen as observed in previous studies by the same author [5].

Table 6. Results of Impact tests of weldments produced using the fillers ERNiCrFe-7 & ERNiCr-3

Welding Process	Toughness (J)			Average
	Trial 1	Trial 2	Trial 3	
Alloy 690	71.3			
ERNiCrFe-7	69	66	70	68.3
ERNiCr-3	65	66	70	67

Figure 11 and 12 shows the impact test specimen and the fracture surface morphology of the weldment.

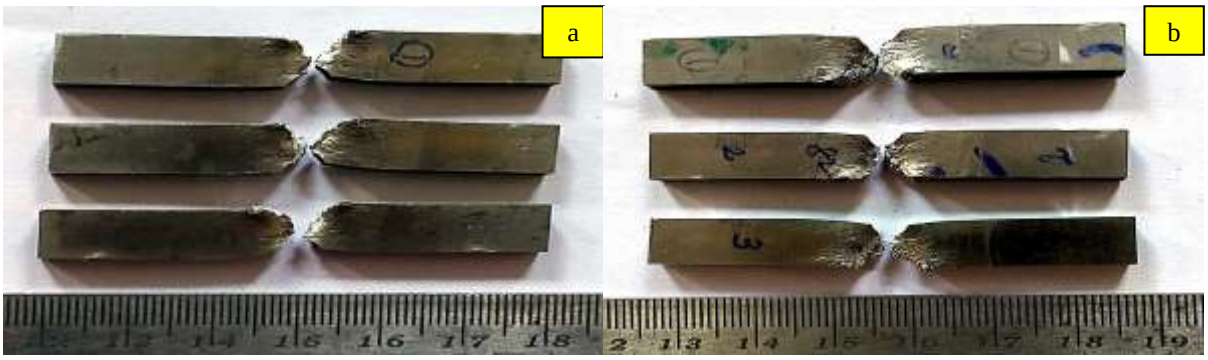

Figure 11. Photographs of impact test of fractured specimen (a) PCGTAW ERNiCrFe-7; (b) PCGTAW ERNiCr-3

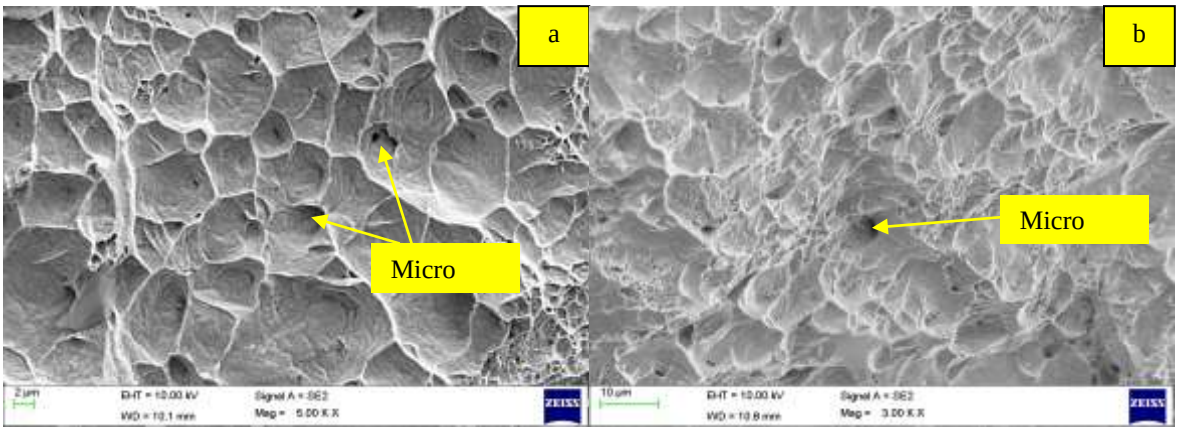

Figure 12. SEM Fractograph of impact failure of PCGTAW (a) ERNiCrFe-7; (b) ERNiCr-3

5. CONCLUSIONS

The experimental analysis on the usage of filler wires for the welding of Inconel 690 weldments using PCGTA welding reveals that the following observations:

1. Macro graph confirms that the weldments were free from defects in the present study. It could also be seen that the adopted process parameters in the present study were also found to be optimum.
2. The micro structure of PCGTA weldment resulted in the fine equiaxed dentritic structure in the weld centre. This could be owing to the faster cooling rate attained in the PCGTA weldment.
3. SEM / EDS confirm the absence of Cr23C6 Cr-rich phases in the inter dentritic regions of the weldment. Segregation of chromium is completely suppressed in the present study.
4. Tensile and Impact test result confirms that the PCGTA weldments fabricated by both the filler wires are stronger than the base metal.

References

[1] S.L. Jeng, H.T. Lee, T.E. Weirich, W.P. Rebach, Microstructual Study of the Dissimilar Joints of Alloy 690 and SUS 304L Stainless Steel, Materials Transactions. 48 (2007) 481–489. doi:10.2320/matertrans.48.481.

[2] Special Metal Data Sheet, Alloy 690, 20alloy%20690.pdf. Accessed 08 August 2018.

[3] H. Lee, T. Kuo, Analysis of microstructure and mechanical properties in alloy 690 weldments using filler metals I-82 and I-52, Science and Technology of Welding and Joining. 4 (1999a) 94–103. doi:10.1179/136217199101537626.

[4] H. Lee, T. Kuo, Effects of niobium on microstructure, mechanical properties, and corrosion behaviour in weldments of alloy 690, Science and Technology of Welding and Joining. 4 (1999b) 245–256. doi:10.1179/136217199101537752.

[5] S. Sivalingam, G. Sureshkannan, Effect of PCGTAW on the Inconel 690 alloy with respect to microsegregation attainment in comparison with the base metal processed with autogenous welding, Materiali in Tehnologije. 53 (2019) 9–15. doi:10.17222/mit.2018.114.

[6] T.-Y. Kuo, H.-T. Lee, Effects of filler metal composition on joining properties of alloy 690 weldments, Materials Science and Engineering: A. 338 (2002) 202–212. doi:10.1016/s0921-5093(02)00063-1.

[7] V. Rajkumar, N. Arivazhagan, Role of pulsed current on metallurgical and mechanical properties of dissimilar metal gas tungsten arc welding of maraging steel to low alloy steel, Materials & Design. 63 (2014) 69–82. doi:10.1016/j.matdes.2014.05.055.

[8] G. P. YU and H. C. YAO: Corrosion, 1990, 46, (5), 391–402.

[9] 'Inconel 690', Huntington Alloys Inc., Huntington, WV, 1980.

[10] L.Rajesh kumar, K.S.Amirthagadeswaran. "Corrosion and wear behaviour of nano Al2O3 reinforced copper metal matrix composites synthesized by high energy ball milling." Particulate Science and Technology, Vol.38 (2) (2020), pp. 228-235, DOI: 10.1080/02726351.2018.1526834.

[11] A. Srikanth, M. Manikandan, Development of welding technique to avoid the sensitization in the alloy 600 by conventional Gas Tungsten Arc Welding method, Journal of Manufacturing Processes. 30 (2017) 452–466. doi:10.1016/j.jmapro.2017.10.014.

[12] B. Arulmurugan, M. Manikandan, Investigations on Microstructure and Corrosion behavior of Superalloy 686 weldments by Electrochemical Corrosion Technique, IOP Conference Series: Materials Science and Engineering. 310 (2018) 012071. doi:10.1088/1757-899x/310/1/012071.

[13] A. Hadadzadeh, M.M. Ghaznavi, A.H. Kokabi, The effect of gas tungsten arc welding and pulsed-gas tungsten arc welding processes' parameters on the heat affected zone-softening behavior of strain-hardened Al–6.7Mg alloy, Materials & Design. 55 (2014) 335–342. doi:10.1016/j.matdes.2013.09.061.

[14] K. Mageshkumar, P. Kuppan, N. Arivazhagan, Characterization of microstructure and mechanical properties of nickel based superalloy 617 by pulsed current gas tungsten arc welding technique, Materials Research Express. 5 (2018) 066541. doi:10.1088/2053-1591/aacb56.

[15] L.Rajesh kumar, A.Saravanakumar, V.Bhuvaneswari, G.Gokul, D.Dinesh kumar, M.P.Jithin karunan. "Optimization of wear behaviour for AA2219-MoS2 metal matrix composites in dry and lubricated condition". Materials Today: Proceedings, vol.27 (3) (2020), pp.2645-2649, https://doi.org/10.1016/j.matpr.2019.11.087

[16] G.J. Ram, A.V. Reddy, K.P. Rao, G. Reddy, J.S. Sundar, Microstructure and tensile properties of Inconel 718 pulsed Nd-YAG laser welds, Journal of Materials Processing Technology. 167 (2005) 73–82. doi:10.1016/j.jmatprotec.2004.09.081.

[17] S. Manikandan, D. Sivakumar, K.P. Rao, M. Kamaraj, Effect of weld cooling rate on Laves phase formation in Inconel 718 fusion zone, Journal of Materials Processing Technology. 214 (2014) 358–364. doi:10.1016/j.jmatprotec.2013.09.006.

[18] M. Manikandan, N. Arivazhagan, M.N. Rao, G. Reddy, Microstructure and mechanical properties of alloy C-276 weldments fabricated by continuous and pulsed current gas tungsten arc welding techniques, Journal of Manufacturing Processes. 16 (2014) 563–572. doi:10.1016/j.jmapro.2014.08.002.

[19] L.Rajesh kumar, K S Amirthagadeswaran. "Variations in the properties of copper-alumina nanocomposites synthesized by mechanical alloying." Materiali in Technologie, 53(1) (2019): 57-63.

[20] A. Raveendra B. V. R. Ravi Kumar; S. Sudhakara Reddy, Micro-Hardness and Mechanical Properties of 5052 Aluminium Alloy Weldments Using Pulsed and Non-Pulsed Current Gas Tungsten ARC Welding, International Journal of Mechanical and Production Engineering Research and Development. 8 (2018) 691–698. doi:10.24247/ijmperddec201871.